Video Article

Resonance Fluorescence of an InGaAs Quantum Dot in a Planar Cavity Using Orthogonal Excitation and Detection

Disheng Chen[1], Gary R. Lander[1], Edward B. Flagg[1]

[1]Department of Physics and Astronomy, West Virginia University

Correspondence to: Edward B. Flagg at Edward.Flagg@mail.wvu.edu

URL: https://www.jove.com/video/56435
DOI: doi:10.3791/56435

Keywords: Engineering, Issue 128, Quantum dot, fluorescence, resonance fluorescence, microcavity

Date Published: 10/13/2017

Citation: Chen, D., Lander, G.R., Flagg, E.B. Resonance Fluorescence of an InGaAs Quantum Dot in a Planar Cavity Using Orthogonal Excitation and Detection. *J. Vis. Exp.* (128), e56435, doi:10.3791/56435 (2017).

Abstract

The ability to perform simultaneous resonant excitation and fluorescence detection is important for quantum optical measurements of quantum dots (QDs). Resonant excitation without fluorescence detection – for example, a differential transmission measurement – can determine some properties of the emitting system, but does not allow applications or measurements based on the emitted photons. For example, the measurement of photon correlations, observation of the Mollow triplet, and realization of single photon sources all require collection of the fluorescence. Incoherent excitation with fluorescence detection – for example, above band-gap excitation – can be used to create single photon sources, but the disturbance of the environment due to the excitation reduces the indistinguishability of the photons. Single photon sources based on QDs will have to be resonantly excited to have high photon indistinguishability, and simultaneous collection of the photons will be necessary to make use of them. We demonstrate a method to resonantly excite a single QD embedded in a planar cavity by coupling the excitation beam into this cavity from the cleaved face of the sample while collecting the fluorescence along the sample's surface normal direction. By carefully matching the excitation beam to the waveguide mode of the cavity, the excitation light can couple into the cavity and interact with the QD. The scattered photons can couple to the Fabry-Perot mode of the cavity and escape in the surface normal direction. This method allows complete freedom in the detection polarization, but the excitation polarization is restricted by the propagation direction of the excitation beam. The fluorescence from the wetting layer provides a guide to align the collection path with respect to the excitation beam. The orthogonality of the excitation and detection modes enables resonant excitation of a single QD with negligible laser scattering background.

Video Link

The video component of this article can be found at https://www.jove.com/video/56435/

Introduction

Resonant excitation of a single quantum emitter combined with fluorescence detection was a long-term experimental challenge mainly due to the inability to spectrally discriminate the weak fluorescence from the strong excitation scattering. This difficulty, however, has been successfully overcome in the past decade by two different approaches: dark-field confocal excitation based on polarization discrimination[1,2,3,4,5], and orthogonal excitation-detection based on spatial mode discrimination[6,7,8,9,10,11,12,13,14]. Both approaches demonstrate a strong capability to significantly suppress laser scattering and thus are widely adopted in various experiments, for example, observation of spin-photon entanglement[5,15,16], demonstration of dressed states[2,7,12,17,18,19,20,21,22,23,24,25,26], and coherent manipulation of confined spins[3,27,28,29,30]. Neither approach can be universally applied to every situation; each is limited to some specific conditions. The dark-field technique utilizes the polarization degree of freedom of photons to suppress the excitation laser scattering. This technique has several advantages. For example, there is no requirement for a well-defined waveguide mode, which enables confocal-only implementation. The confocal implementation allows for circularly polarized excitation and possibly tighter focus of the excitation beam at the quantum emitter, resulting in higher excitation intensity. However, this polarization-selective method restricts the detection polarization to be orthogonal to the excitation polarization, and thus prevents a complete characterization of the polarization properties of the fluorescence. In comparison, spatial mode discrimination preserves the complete freedom of detection polarization by utilizing the orthogonality between the propagation modes of excitation and detection beams to suppress the laser scattering[4]. The constraints of this technique are the necessity of a waveguide structure in the sample to provide an excitation mode orthogonal to the detection mode, and the restriction of the excitation polarization to be perpendicular to the propagation direction of the beam.

Here, we demonstrate a protocol for constructing a free-space-based orthogonal excitation-detection setup for resonance fluorescence experiments. Compared to the pioneering work on spatial mode discrimination where an optical fiber was used to couple light into the cavity[6], this protocol provides a solution in free space, and does not require kinetic components to mount either the sample or the fiber in cryostat. Fine control of the directions of the excitation beam and the detection path are manipulated by optics external to the cryostat, while aspheric singlet lenses act as focusing objectives inside the cold region of the cryostat. We provide representative images of the key alignment steps in the process of achieving resonant excitation and detection of fluorescence from a single quantum dot.

The sample used for this demonstration is grown by molecular beam epitaxy (MBE). The InGaAs quantum dots (QDs) are embedded in a GaAs spacer that is bounded by two distributed Bragg reflectors (DBRs), as shown in the zoom-in view of the sample in **Figure 1**. The GaAs spacer

Copyright © 2017 Journal of Visualized Experiments

between the DBRs acts as a waveguide, where the excitation beam is confined by total internal reflection. The DBRs also act as high-reflectivity mirrors for wavevectors that are nearly normal to the sample plane. This forms a Fabry-Perot mode to which the QDs couple when emitting fluorescence. The Fabry-Perot mode must be resonant with the emission wavelength λ of the QDs, which requires the GaAs spacer to be an integer multiple of λ/n, where n is the index of refraction of GaAs. For this demonstration, the thickness of the GaAs spacer is chosen to be 4λ/n, which is approximately 1 μm, so as to be near the diffraction limited spot size of the incident excitation beam. A narrower spacer would result in a lower coupling efficiency of the excitation beam into the waveguide mode.

The experimental setup is shown in **Figure 1**. To maximize the coupling efficiency, an aspheric single-lens objective E_{obj} with numerical aperture NA=0.5 and focal length of 8 mm is chosen to focus the excitation beam onto the cleaved face of the sample. The function of the Keplerian telescope (composed of lens pair E1 and E2) in the excitation path is two-fold: (1) to fill the aperture of the excitation objective E_{obj} so the excitation beam is tightly focused for better mode-matching to the waveguide (in this realization the collimated beam diameter is 2.5 mm), and (2) to provide three degrees of freedom to maneuver the focal point of the excitation beam at the cleaved face of the sample. Lens E1 is mounted on an X-Y translational mount that provides the two degrees of freedom to shift the excitation spot freely in the plane of the cleaved sample face. Lens E2 is mounted on a non-rotating zoom housing which provides the freedom to choose the depth of the focal point in the sample. These three degrees of freedom allow us to optimize the resonant excitation of a single QD without requiring movement of the sample itself.

In the fluorescence collection path, a similar lens configuration (L_{obj}, L1, and L2) is used to allow detection of fluorescence from different parts of the sample. The light from the sample is focused by one of two tube lenses onto either an IR-sensitive camera (L_{cam}) or the entrance slit of the spectrometer (L_{spec}). Motion of L1 along the z-axis adjusts the focus of the image, and lateral translation of L2 causes the image to scan across the plane of the sample. The focal lengths of L1 and L2 are equal so their magnification is unity. This is done to maximize the range L2 can be translated before vignetting occurs.

To facilitate alignment and location of a QD, a home-built illuminator based on Kohler illumination is incorporated into the setup, as shown in **Figure 1**. The purpose of Kohler illumination is to provide uniform illumination to the sample and ensure that an image of the illumination light source is not visible in the sample image. The lens configurations of both the illuminator and the collection path are carefully designed to separate the conjugate image planes of the sample and the light source. Every lens in the collection path is separated from its neighbors by the sum of their focal lengths. This ensures that wherever the sample image is in focus – such as at the sensor of the camera – the light source image is completely defocused. Similarly, where the light source image is in focus – such as at the back focal plane of the objective – the sample image is completely defocused. The light source is a commercial light emitting diode (LED) emitting at 940 nm. The aperture diaphragm enables the adjustment of the illumination intensity, and the field diaphragm determines the field of view to be illuminated. The keys to realizing uniform illumination are to set the distance between lens K4 and L2 to be the sum of the focal lengths of the two lenses, and to ensure that the aperture of L_{obj} is not overfilled by the illumination. In this protocol, the illumination is also used to optimize the distance between L_{obj} and the sample.

The objective L_{obj} and either tube lens provides a magnification of 20x on the camera or the spectrometer. The lens pair L3 and L4 between L_{obj} and L_{spec} forms another Keplerian telescope that provides an extra 4x magnification to the image on the charge-coupled device (CCD) of the spectrometer. The addition of lenses L3 and L4 results in a total magnification of 80x, which is necessary to spatially distinguish fluorescence from nearby QDs. L3 and L4 are mounted on flipping mounts to facilitate switching of the magnification because 20x magnification provides a larger field of view on the sample.

To overlap the field of view of the collection path with the path of the excitation beam through the waveguide, the emission from the continuum of the quantum dot wetting layer is helpful. One can determine the emission wavelength of the wetting layer by measuring the emission spectrum of the sample under above band-gap excitation. For our sample, wetting layer emission occurs at approximately 880 nm at 4.2 K. By coupling a *cw* laser beam at 880 nm into the waveguide of the sample, one can observe a streak pattern formed by the PL from the wetting layer, which is shown in the accompanying video. The streak reveals the propagation path of the excitation light that has been coupled into the waveguide. The presence of this streak combined with the ability to image the surface of the sample makes alignment straightforward.

Protocol

Caution: Please be aware of the possible dangers of laser scattering during the alignment. Wear proper safety goggles for protection. To facilitate the alignment process, an infrared viewer (IR-viewer) is necessary. An IR-sensitive fluorescent card is also helpful but not necessary.

1. Sample Preparation

1. Use a diamond scribe to make a miniscule scratch on the edge of the top surface of the sample at the desired location of the cleave. Use two pairs of flat-ended tweezers to hold the sample on both sides of the scratch. Apply an outward-rotating torque with the tweezers and the sample will cleave.
   NOTE: A long scratch is unnecessary to promote cleaving, and it will likely cut through the waveguide layer making light coupling impossible. The cleaved face is delicate enough that any touch on its surface might damage the waveguide face.
2. Attach the cleaved sample piece onto a copper sample plate using thermally conductive silver paint or silver epoxy.
   NOTE: The cleaved face should be flush with the edge of the mounting plate so that the excitation laser will hit the sample face without interference.
3. Mount the copper plate in the cryostat so that both the cleaved face and the sample surface are optically accessible through the cryostat windows.

2. Alignment of Resonant Excitation Path

NOTE: To maximize the coupling efficiency into the waveguide, the profile of the incident excitation beam has to be matched with that of an imaginary backwards propagating beam exiting the waveguide.

1. **Coarse alignment of excitation laser beam to the cleaved face of the sample.**
    1. Use the degrees of freedom of optical fiber coupler FC0 and mirror M0 to direct the excitation beam onto the cleaved face of the sample before the excitation lenses are installed.
    2. Level the excitation beam horizontally both with respect to the optical table and with respect to the plane of the sample.

2. **Installation of excitation objective** E_{obj}
    1. Put the aspheric lens E_{obj} in a translational mount with three degrees of translational freedom. Center E_{obj} on the laser and set the height of E_{obj} to be the same as the center of the sample.
    2. Set up a white paper screen behind the sample along the excitation path. Use an IR-viewer to observe a bright spot on the paper due to the laser light passing by the sample.
    3. Slide E_{obj} towards the sample slowly until a clear silhouette image of the sample can be seen on the paper. Adjust the height and lateral position of E_{obj} to center the silhouette at the middle of the bright spot.
    4. Keep sliding E_{obj} towards the sample slowly, and the silhouette image on the screen experiences a magnification. Meanwhile, adjust the lateral position of E_{obj} (left/right) to compensate the horizontal shifting of the silhouette image.
    NOTE: During the slow movement of E_{obj} to the sample, diffraction fringes will start to appear at some point. This provides a new reference to put the focused spot at the surface layer of the sample.
    5. Keep sliding E_{obj} towards the sample slowly. At each location of E_{obj}, shift E_{obj} left/right increase the fringe spacing until there is only one fringe visible to look for fringes on the screen.
    Note: There will be two groups of fringes, one to the left and one to the right of the sample surface.
    6. Locate Slide E_{obj} Eobj at a position that minimizes the number of fringes visible.

3. **Alignment of telescope lenses E1 and E2**
    1. Insert lenses E1 and E2 into the excitation path centered on the laser beam. Position E2 separated from E_{obj} by the sum of their focal lengths. Set the separation between E1 and E2 to be the sum of their focal lengths, *e.g.*, $f_1 + f_2 = 150$ mm.
    2. Observe the silhouette and diffraction pattern on the paper with an IR-viewer. Adjust the height of E1 to center the silhouette at the center of the bright laser illumination spot.
    3. Slide E2 towards or away from E1 while adjusting the lateral position of E1. Secure E1 and E2 at positions that both fringe groups either disappear or show a minimum number of fringes in the view.
    4. Insert a vertically oriented polarizer POL before E1, and center it on the excitation beam.
    Note: Some polarizers have a slight wedge angle, in which case the excitation beam will experience an angular deviation. Use E1 and E2 to compensate this deviation.

3. Alignment of Photoluminescence Collection Path

NOTE: The performance of the imaging system built in the collection path is mostly determined by the precision of the positioning of L_{obj} because of its short focal length (f_{obj} = 10mm, NA=0.55). Two general steps are involved in the alignment of L_{obj}: coarse alignment by using a HeNe laser, and fine tweaking by using the illuminator and the bulk exciton emission of GaAs. These alignment steps are performed with the sample at room temperature.

1. **Alignment of the above band-gap (HeNe) excitation path and installation of the camera:**
    1. Couple an above band-gap laser beam (HeNe) into a single mode fiber.
    2. Direct the output beam from the fiber collimator FC1 onto the sample via a mirror M3.
    3. Tilt FC1 horizontally to center the laser spot on the sample about 1 mm away from the cleaved edge. Tilt M3 horizontally to shift the back reflection of the laser beam to be just above or below the incident beam. Repeat this process several times till meeting both criteria.
    4. Tilt FC1 and M3 vertically to level the HeNe beam with respect to the optical table and keep it directed at the sample.
    5. Use the IR viewer to locate both the resonant laser and the HeNe laser spots on the sample. Check that the center of the HeNe laser spot is at the same height as the resonant laser spot. If not, use FC1 and M3 to match the beam heights while keeping the HeNe beam level with the table.
    6. Insert the non-polarizing beam splitter cube (90:10), NPBS, into the HeNe path. Center the cube in the incident HeNe beam.
    7. Locate two beams at the beam splitter output to the collection path, one from reflection from the sample, and one from internal reflection within the cube.
    8. Rotate the cube by a small angle (~5 degrees) such that the two beams can be easily separated at the exit. The light reflected off the sample surface can be used as a crude guide to align the camera.
    NOTE: The direction of the internally reflected beam will not change when the cube is rotated about the vertical axis.
    9. Level the cube with respect to the optical table by ensuring the HeNe beam corresponding to the internal reflection inside the cube is at the same height as the incoming beam.
    10. Put an IR-sensitive camera in the path of the back reflected HeNe beam. Use a tube lens L_{cam} with a focal length of 200 mm to focus the sample image onto the camera.
    NOTE: A home-built tube system is used to house the lens L_{cam}, as shown in **Figure 1**, which prevents stray room light from being detected by the camera.
    11. Set up an 800 nm long-pass filter, F1, in front of L_{cam} to filter out the HeNe light, which allows the observation of PL from the sample with the camera.

2. **Installation and optimization of the position of lens** L_{obj}
    1. Put the aspheric lens L_{obj} in a translational mount with three degrees of translational freedom. Center L_{obj} on the HeNe laser and set the separation from the sample to be the focal length, f_{obj} = 10 mm.
    2. Set up lens pair L1 and L2 ($f_1 = f_2 = 50$ mm) by using an X-Y translational mount where one side is fixed and the other side is movable in the lateral plane controlled by micrometers.

NOTE: Lens L2 goes into the movable side of the mount. L1 is held by a lens tube and attached to the fixed side of the mount. The tube system provides the freedom to adjust the distance between the two lenses by screwing in/out the lens tube holding L1 along the optical axis.

3. Set the distance between the two lenses to be 100 mm. Set L2 at the center of the mount by adjusting the micrometers.
4. Insert the L1 and L2 lens combo into the HeNe path between NPBS and the cryostat. Set the distance between L1 and L_{obj} to be f_{obj} + f_1. Center L1 and L2 on the incident HeNe light.
5. Insert the illuminator and pellicle into the collection path as shown in **Figure 1**. Set the distance between lens K4 and L2 to be the sum of their focal lengths.
6. Center the illumination beam on L2 by adjusting the angle of the illuminator.
7. Adjust the angle of the pellicle to center the back reflected illumination light visible in the camera image to the PL spot caused by HeNe excitation.
   NOTE: For the purpose of alignment, one can close the field diaphragm to locate the center of the illuminated area.
8. Using only the illuminator light, find a surface defect or dust on the sample by looking at the camera. Search other parts of the sample as needed by moving L2 laterally.
9. Slightly tap L_{obj} in/out along the optical axis to make the edge of the defect or dust sharpest.
10. Shift L2 back to the center of the mount.
11. View the HeNe-excited PL spot on the camera, and move L_{obj} horizontally so that the PL spot is 1-2 mm from the cleaved edge of the sample.
    NOTE: For a distance less than 1 mm, the laser scattering from the cleaved edge of the sample would be collected by objective L_{obj}. While for a distance too far from the cleaved face, the excitation beam can experience attenuation before reaching the QD, which reduces the maximum excitation power available.
12. Shift L2 horizontally till the cleaved edge of the sample is shown on the camera under illumination.
13. Slowly shift L_{obj} vertically to look for a bright laser spot on the cleaved edge of the sample, which is caused by the scattering of the resonant excitation beam at the cleaved face of the sample.
14. Level the PL spot caused by HeNe excitation to the bright laser spot on the cleaved edge of the sample.

3. **Realignment of the HeNe excitation path with respect to the new location of L_{obj}.**
   NOTE: To maximize scannable area and minimize vignetting, it is necessary to re-center the excitation optics and the excitation beam with respect to the location of L_{obj}.
   1. Remove L1 and L2. Center the excitation beam on L_{obj} while ensuring the beam is in the surface normal direction of the sample.
   2. Center L2 on the mount. Center both L1 and L2 on the incident excitation beam. Set the distance between L1 and L_{obj} to be the sum of the two focal lengths, *i.e.*, f_1 + f_{obj}.
   3. Reposition L_{cam} such that it is centered on reflected HeNe beam. Reposition the camera such that the HeNe excited PL (use a long-pass filter) is centered on the image.
   4. Adjust the angle of the illuminator and the pellicle to center the illumination light on L2 and on the PL spot caused by HeNe excitation.

4. **Alignment of mirrors M1 and M2.**
   NOTE: A laser directed backwards through the spectrometer will facilitate alignment.
   1. Monitor the HeNe-excited PL from the sample at the camera. Center an iris (Iris A) on the PL between the pellicle and M1.
   2. Center lens L_{spec} on the reverse beam and place it one focal length f_{spec} away from the entrance slit of the spectrometer.
   3. Send the reverse beam from the spectrometer to the sample by reflecting off of two mirrors, M1 and M2.
   4. Set up another iris (Iris B) between M2 and L_{spec} and center it on the reverse beam.
   5. Steer M2 to center the reverse beam on Iris A. Steer M1 to center the PL on Iris B. Repeat this process several times until both criteria are satisfied.
   6. Locate the center of the entrance slit (30 µm width) of the spectrometer on the CCD by monitoring the zero-order diffraction of the room light.
   7. Open the entrance slit of the spectrometer. By using an 800 nm long pass filter, the PL from the sample under HeNe excitation can be observed on the CCD.
   8. Steer M1 to center this spot at the entrance slit of the spectrometer and at the middle height of the CCD, and steer M2 to center the reverse beam on Iris A. Repeat this process several times until both criteria are met.
   9. Alignment of lens pair L3 and L4: Position L3 in the PL collection path at a location that is f_2 + f_3 away from lens L2. Place L4 into the collection path separated from L3 by the sum of their focal lengths, f_3 + f_4. Adjust the lateral position of L4 to center the PL spot on the CCD.

4. Overlap of the PL Collection Path with respect to the Resonant Excitation Path

1. Cool down the sample to 4.2 K. With the above-band excitation, use the spectrometer to pinpoint the emission wavelength of the wetting layer (typically around 880 nm).
2. Set up an 800 nm long-pass filter F1 in front of L_{cam} to block the HeNe light. With the help of the illuminating light, shift L2 horizontally to locate the cleaved edge of sample on the camera.
3. Set the side excitation wavelength to be resonant with the wetting layer. Locate a bright scattering spot at the cleaved edge of the sample on the camera.
4. Observe a "streak pattern" of photoluminescence on the camera by adjusting the lateral position of E1. Maximize the intensity of the streak by shifting E1 laterally.
   NOTE: The "streak" is the wetting layer emission, which implies that the excitation beam is coupled into the waveguide of the sample.
5. Adjust E1 vertically to move the streak to overlap with the PL spot caused by the HeNe excitation.
6. Record the intensity of the wetting layer PL. Adjust E2 in one direction, then re-optimize the position of E1; again record the intensity of the PL and compare to the earlier value.

Copyright © 2017 Journal of Visualized Experiments

7. If the intensity has increased, repeat the adjustment of E2 in the same direction. If the intensity has decreased, then reverse the adjustment of E2. Repeat this procedure to find the optimum positions for both E1 and E2.

5. Resonant Excitation of a Single Quantum Dot

NOTE: There are two possible approaches to realize resonant excitation of a single QD: (1) tune the excitation frequency of the laser to match a specific QD resonance; or (2) scan the laser frequency across the resonance energies of the QD ensemble until resonance fluorescence from a single QD is observed.

1. **Method (1) - Targeted excitation:**
    1. Set the spectrometer to monitor the first-order diffraction at the center of the emission wavelength of the QD ensemble under above band-gap excitation. Open the entrance slit of the spectrometer.
    2. Adjust the power of the above-band excitation until a glowing background appears due to excitation of the continuum tail of the wetting layer states. Close the entrance slit to 30 μm.
    3. Shift L2 laterally to find a suitable QD - for example, the brightest one in view. Record the wavelength of the QD λ_{QD} as measured by the spectrometer.
    4. Tune the wavelength of the resonant excitation laser to be the same value as λ_{QD}.
    NOTE: Often, the spectrometer can pick up the weak signal of the scattering of the resonant excitation laser from the optics. If not, direct a split-off of the excitation beam into the spectrometer.
    5. Maximize the QD's PL intensity at on the CCD by fine tuning the frequency of the excitation laser.
    NOTE: For some QDs, a small amount of HeNe light is needed to allow the QD to be resonantly excited[10,31,32]. The required HeNe laser power is usually so low - a few hundred nanowatts - that no fluorescence caused solely by this HeNe beam can be detected by the CCD.
    6. Maximize the PL intensity of the QD by adjusting the height and the lateral position of lens E1 and the axial position of lens E2. Jointly optimize the positions of lenses E1 and E2 to maximize the intensity of the resonance fluorescence from the QD.

2. **Method (2) - Spectral searching:**
    1. Set the spectrometer to monitor the first-order diffraction at the center of the emission wavelength of the QD ensemble. Open the entrance slit of the spectrometer.
    2. Tune the frequency of the excitation laser across the energy range of the QD ensemble. A resonantly excited QD will appear on the CCD as a dot surrounded by couple of Airy rings. Pick a QD that is bright.
    3. Maximize its PL intensity by fine tuning the wavelength of the excitation laser.
    4. Maximize the PL intensity of the dot by adjusting the height and the lateral position of E1and the axial position of lens E2. Jointly optimize the positions of lenses E1 and E2 to maximize the intensity of the resonance fluorescence from the QD.

Representative Results

Figure 1 shows one particular realization of the necessary equipment to accomplish resonant excitation of a single quantum dot. Other realizations are possible, but the critical components are: an excitation path to couple to the waveguide; a collection path to guide fluorescence to detectors; a confocal excitation path to excite along the collection path; and an illumination path to enable imaging of the sample surface.

Two representative RPLE spectra are shown in **Figure 2**. They are collected from a neutral QD [**Figure 2(a) and (b)**] and a charged QD [**Figure 2(c) and (d)**]. The exact charge state of the charged QD cannot be determined by examining the spectrum. To achieve the best signal-to-noise ratio, laser scattering must be kept to a minimum. The rightmost images in **Figure 2(a) and (c)** show the scattering background when the excitation laser is far-detuned from resonance. The laser scattering is much weaker than the QD fluorescence, but to illustrate the typical patterns of scattering, the images have been enhanced by 284 and 23 times, respectively. If these images are encountered in the alignment, it implies that a strong laser scattering is present. Multiple causes can lead to this result, such as misalignment of coupling into the waveguide, scratches on the cleaved face of the waveguide, a field of view too close to the cleaved edge of the sample, *etc*. Detailed discussions on each point are provided in the Discussion part of this protocol.

The image of a resonantly excited QD in a planar microcavity will typically have central disk with rings around it as shown in **Figure 3**. This pattern results from the coupling of the QD to the plane-wave eigenmodes of the cavity, whose propagation directions are wavelength dependent[33]. Thus, fluorescence of a single wavelength emerges from the cavity in a hollow cone whose apex angle is determined by the wavelength of the emission. When this light is collimated by the objective and focused by the tube lens, the image formed has the ring-like structure evident in **Figure 2** and **Figure 3**. The radii of the rings and disk will be determined by the apex angle and thus the emission wavelength. The smaller the emission wavelength, the larger the apex angle, and the smaller the radii. The smallest possible apex angle is zero, which means there is a long-wavelength cutoff for emission that can escape the cavity. The largest possible apex angle is determined by the NA of the objective lens, which means there is a short-wavelength cutoff for emission that can be collected by the optical system. An objective with a larger NA - or the addition of a solid immersion lens - would extend this low end of the collection band to shorter wavelengths. On the other hand, the long wavelength end of the collection band cannot be modified except by changing the sample structure. **Figure 3** shows images of fluorescence from QDs with different emission wavelengths ranging from the minimum up to the cutoff wavelength.

Copyright © 2017 Journal of Visualized Experiments

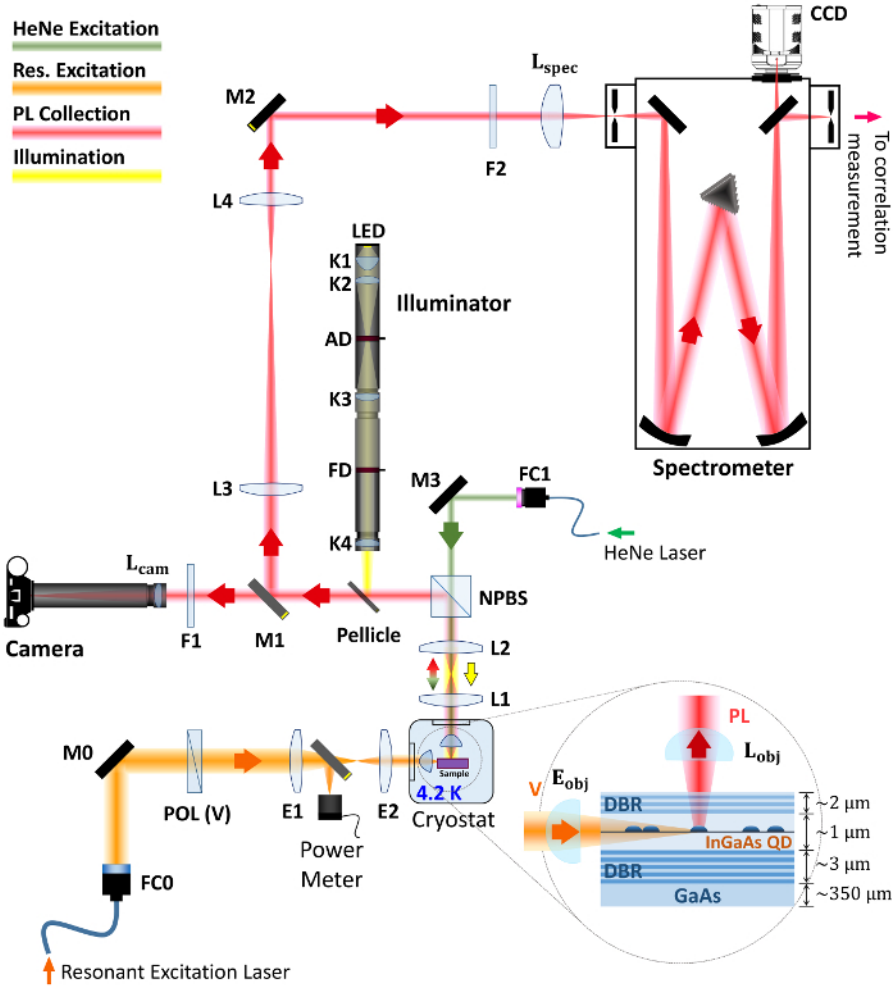

Figure 1. Schematic of the experiment.
Resonant excitation of a single QD is realized by coupling a narrow linewidth (1 MHz) *cw* laser beam into the waveguide of the sample, as depicted by the orange path. The photoluminescence of the sample is collected from the Fabry-Perot mode, following the red path. A Helium-Neon (HeNe) laser provides the above band-gap excitation confocally, following the green path. A home-built illuminator provides uniform illumination of the sample surface with 940 nm light, as depicted by the yellow path. Note that the schematic is not to scale. FC: fiber coupler; AD: aperture diaphragm; FD: field diaphragm; POL: polarizer; F: long-pass filter; NPBS: non-polarizing beam splitter cube; DBR: distributed Bragg reflector; CCD: charge-coupled device; LED: light-emitting diode. Please click here to view a larger version of this figure.

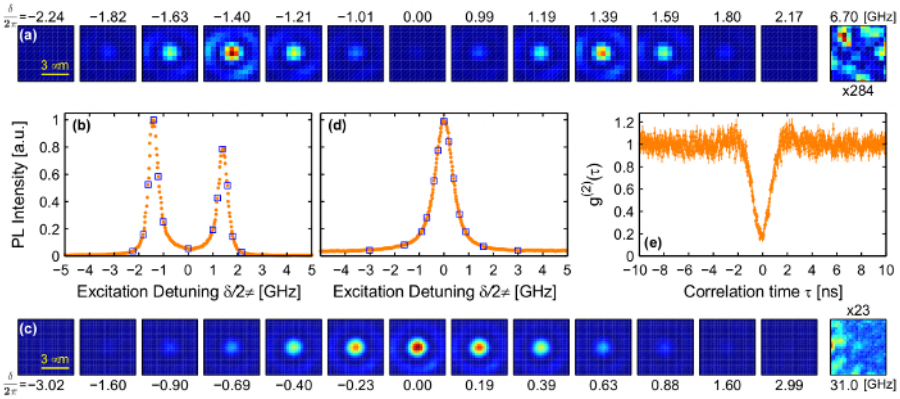

Figure 2. Resonance fluorescence of a single quantum dot.
(a) Images of fluorescence of a neutral quantum dot at different detunings, indicated in linear frequency on the top of each image. Zero detuning corresponds to 927.8597 nm. (b) RPLE spectrum of the same neutral QD, by integrating the PL intensity in a circular area with a diameter of 8 pixels around the center. (c) Images of fluorescence of a charged QD at different detunings, indicated in linear frequency at the bottom of each image. Zero detuning corresponds to 927.653 nm. (d) RPLE spectrum of the same charged QD, by integrating the PL intensity in a circular area of a diameter of 12 pixels around the center. (e) Second-order correlation measurement of the neutral QD in (a) under resonant excitation at the low-energy peak. The right-most frames in (a) and (c) are the far-detuned excitation images, with the intensity multiplied by 284 and 23, respectively, to show the low laser scattering background. Note that the color scale for (a) and (c) are different but shared among the individual sub-plots. The normalized RPLE intensity in (b) and (d) is depicted by orange dots, while blue squares indicate the data corresponding to the images shown in (a) and (b), respectively. Please click here to view a larger version of this figure.

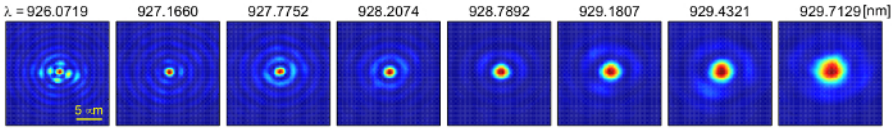

Figure 3. Resonance fluorescence from eight different dots at different wavelengths in the cavity mode.
The resonance wavelength is indicated on the top of each image. Please click here to view a larger version of this figure.

Discussion

The critical steps in the protocol are: the mode-matching and alignment of the excitation beam to the waveguide mode; and proper alignment and focusing of the collection optics. The most difficult parts of these steps are the initial alignment; optimizing the coupling of an already aligned setup is relatively straightforward. Overlapping the collection and excitation areas is a step that is simple with the ability to image the sample on the camera, but is very difficult without this capability. In order to have high-quality imaging, proper Kohler illumination is critical. The topic of Kohler illumination is outside the scope of this protocol, but is a well-known concept in microscopy and is comprehensively discussed in the published literature[34,35].

The lens focal lengths noted here are typical, but not required. Different cryostats and other factors may impose additional or different requirements on the optics arrangement. In such a case, proper choices of lens focal lengths during design is key to satisfy the requirements of mode-matching in the excitation path and Kohler illumination in the collection path. Kohler illumination will be satisfied if lenses are separated by the sum of their focal lengths. Proper mode-matching into the waveguide requires as high an NA as possible, which means the beam must fill the aperture of E_{obj}. The objective sits in a homemade dovetail rail XYZ mount that is movable only at room temperature because it is located inside the code space of the cryostat. This close-to-sample position allows the use of a large NA lens while minimizing the thermal variation in the lens mounts, which increases mechanical stability. The objectives in this case are aspherical singlet lenses due to space constraints. If more space is available, commercial multi-lens objectives could be used instead to improve imaging quality, NA, and magnification. The experimental setup could be extended to allow confocal resonant or near-resonant excitation by replacing M3 with a dichroic mirror and directing an excitation beam through both the dichroic and the beam splitter NPBS.

If the laser background is too strong, poor coupling of the excitation beam into the waveguide is a possible cause. The coupling can be reduced by roughness, scratches, or contamination on the cleaved face due to improper handling. The face that will be coupled to must not be touched by anything. It is possible but difficult to clean the cleaved face of contamination, but roughness and scratches are permanent. If surface quality is an issue, a different location on the cleaved face can be tried, but a fresh cleave may be necessary. Strong laser scattering background can also be caused by the uncoupled portion of excitation light scattering from dust on the surface of the sample. Another possibility is that the field of view is too close to the edge of the sample and light scattering from edge is entering the collection path. Finally, it may be that the laser power is just too high. Typically, the excitation laser power is in the range of 0.5 to 10 μW measured at the power meter shown in **Figure 1**. Aside from reducing sources of laser scattering, the scattering can be filtered out by adding a horizontal polarizer in the collection path. However, to see the QD fluorescence in this situation requires a QD whose dipole moment is not aligned to the vertical direction.

The excitation polarization is limited to only one choice; in this case it is vertical polarization. This is because of three constraints. First, the propagation direction of the excitation beam is constrained to be within the sample plane. Second, the polarization must be perpendicular to the propagation direction. Third, the QD dipole moments lie in the sample plane. If, as in this case, the excitation beam propagates horizontally, then the only choice of polarization that can excite the QDs is vertical. In contrast, the detection polarization has no constraints placed on it because

the suppression of laser scattering is mainly accomplished by confinement of the laser within the waveguide mode[11]. Another limitation is that this excitation scheme requires a waveguide to guide the light to the quantum dot, a structure that may not be feasible for all samples. Compare this to the dark-field confocal excitation technique[1], which uses crossed polarizers to suppress the laser scattering. In that case, the excitation can use arbitrary polarization, but the detection polarization must be orthogonal.

Single quantum dots under resonant excitation have been demonstrated to be excellent single photon sources with high brightness, narrow linewidth, and high indistinguishability[36]. This protocol provides a feasible approach to harness these exceptional properties of the self-assembled QD system for various applications, such as quantum information and linear optical quantum computing. Furthermore, photons entangled with either another photon or an electron spin will require collection without regard to polarization, which is a feature of this method.

Disclosures

The authors have nothing to disclose.

Acknowledgements

The authors would like to acknowledge Glenn S. Solomon for providing the sample. This work was supported by the National Science Foundation (DMR-1452840).

References

1. Kuhlmann, A. V. *et al.* A dark-field microscope for background-free detection of resonance fluorescence from single semiconductor quantum dots operating in a set-and-forget mode. *Rev. Sci. Instrum.* **84** (7), 073905 (2013).
2. Vamivakas, N. A., Zhao, Y., Lu, C.-Y., & Atatüre, M. Spin-resolved quantum-dot resonance fluorescence. *Nat. Phys.* **5** (3), 198-202 (2009).
3. Vamivakas, A. N. *et al.* Observation of spin-dependent quantum jumps via quantum dot resonance fluorescence. *Nature.* **467** (7313), 297-300 (2010).
4. Houel, J. *et al.* Probing Single-Charge Fluctuations at a GaAs/AlAs Interface Using Laser Spectroscopy on a Nearby InGaAs Quantum Dot. *Phys. Rev. Lett.* **108** (10), 107401 (2012).
5. Gao, W. B., Fallahi, P., Togan, E., Miguel-Sanchez, J., & Imamoglu, A. Observation of entanglement between a quantum dot spin and a single photon. *Nature.* **491** (7424), 426-430 (2012).
6. Muller, A. *et al.* Resonance Fluorescence from a Coherently Driven Semiconductor Quantum Dot in a Cavity. *Phys. Rev. Lett.* **99** (18), 187402 (2007).
7. Flagg, E. B. *et al.* Resonantly driven coherent oscillations in a solid-state quantum emitter. *Nat. Phys.* **5** (3), 203-207 (2009).
8. Konthasinghe, K. *et al.* Coherent versus incoherent light scattering from a quantum dot. *Phys. Rev. B.* **85** (23), 235315 (2012).
9. Peiris, M., Konthasinghe, K., Yu, Y., Niu, Z. C., & Muller, A. Bichromatic resonant light scattering from a quantum dot. *Phys. Rev. B.* **89** (15), 155305 (2014).
10. Chen, D., Lander, G. R., Krowpman, K. S., Solomon, G. S., & Flagg, E. B. Characterization of the local charge environment of a single quantum dot via resonance fluorescence. *Phys. Rev. B.* **93** (11), 115307 (2016).
11. Chen, D., Lander, G. R., Solomon, G. S., & Flagg, E. B. Polarization-Dependent Interference of Coherent Scattering from Orthogonal Dipole Moments of a Resonantly Excited Quantum Dot. *Phys. Rev. Lett.* **118** (3), 037401 (2017).
12. Ge, R.-C. *et al.* Mollow quintuplets from coherently excited quantum dots. *Opt. Lett.* **38** (10), 1691 (2013).
13. Proux, R., Maragkou, M., Baudin, E., Voisin, C., Roussignol, P., & Diederichs, C. Measuring the Photon Coalescence Time Window in the Continuous-Wave Regime for Resonantly Driven Semiconductor Quantum Dots. *Phys. Rev. Lett.* **114** (6), 067401 (2015).
14. Robertson, J. *et al.* Polarization-resolved resonant fluorescence of a single semiconductor quantum dot. *Appl. Phys. Lett.* **101** (25), 251118 (2012).
15. De Greve, K. *et al.* Quantum-dot spin-photon entanglement via frequency downconversion to telecom wavelength. *Nature.* **491** (7424), 421-425 (2012).
16. Schaibley, J. R. *et al.* Demonstration of Quantum Entanglement between a Single Electron Spin Confined to an InAs Quantum Dot and a Photon. *Phys. Rev. Lett.* **110** (16), 167401 (2013).
17. Gerardot, B. D. *et al.* Dressed excitonic states and quantum interference in a three-level quantum dot ladder system. *New J. Phys.* **11** (1), 013028 (2009).
18. Hargart, F. *et al.* Cavity-enhanced simultaneous dressing of quantum dot exciton and biexciton states. *Phys. Rev. B.* **93** (11), 115308 (2016).
19. Jundt, G., Robledo, L., Högele, A., Falt, S., & Imamoglu, A. Observation of dressed excitonic states in a single quantum dot. *Arxiv preprint cond-mat/0711.4205v1.* at <http://arxiv.org/PS_cache/arxiv/pdf/0711/0711.4205v1.pdf> (2007).
20. Kim, H., Shen, T. C., Roy-Choudhury, K., Solomon, G. S., & Waks, E. Resonant Interactions between a Mollow Triplet Sideband and a Strongly Coupled Cavity. *Phys. Rev. Lett.* **113** (2), 027403 (2014).
21. Unsleber, S. *et al.* Observation of resonance fluorescence and the Mollow triplet from a coherently driven site-controlled quantum dot. *Optica.* **2** (12), 1072 (2015).
22. Xu, X. *et al.* Coherent Optical Spectroscopy of a Strongly Driven Quantum Dot. *Science.* **317** (5840), 929-932 (2007).
23. Muller, A., Fang, W., Lawall, J., & Solomon, G. S. Emission Spectrum of a Dressed Exciton-Biexciton Complex in a Semiconductor Quantum Dot. *Phys. Rev. Lett.* **101** (2), 027401 (2008).
24. Roy-Choudhury, K., & Hughes, S. Quantum theory of the emission spectrum from quantum dots coupled to structured photonic reservoirs and acoustic phonons. *Phys. Rev. B.* **92** (20), 205406 (2015).
25. Ulhaq, A., Weiler, S., Ulrich, S. M., Roßbach, R., Jetter, M., & Michler, P. Cascaded single-photon emission from the Mollow triplet sidebands of a quantum dot. *Nat. Photonics.* **6** (4), 238-242 (2012).
26. Ulrich, S. M. *et al.* Dephasing of Triplet-Sideband Optical Emission of a Resonantly Driven InAs/GaAs Quantum Dot inside a Microcavity. *Phys. Rev. Lett.* **106** (24), 247402 (2011).

Copyright © 2017 Journal of Visualized Experiments

27. Atature, M., Dreiser, J., Badolato, A., Hogele, A., Karrai, K., & Imamoglu, A. Quantum-dot spin-state preparation with near-unity fidelity. *Science*. **312** (5773), 551-553 (2006).
28. Kroner, M. *et al.* Resonant two-color high-resolution spectroscopy of a negatively charged exciton in a self-assembled quantum dot. *Phys. Rev. B.* **78** (7), 075429 (2008).
29. Press, D., Ladd, T. D., Zhang, B., & Yamamoto, Y. Complete quantum control of a single quantum dot spin using ultrafast optical pulses. *Nature.* **456** (7219), 218-221 (2008).
30. Sun, S., & Waks, E. Single-shot optical readout of a quantum bit using cavity quantum electrodynamics. *Physical Review A.* **94** (1), 012307 (2016).
31. Metcalfe, M., Solomon, G. S., & Lawall, J. Heterodyne measurement of resonant elastic scattering from epitaxial quantum dots. *Appl. Phys. Lett.* **102** (23), 231114 (2013).
32. Nguyen, H. S. *et al.* Optically Gated Resonant Emission of Single Quantum Dots. *Phys. Rev. Lett.* **108** (5), 057401 (2012).
33. Benisty, H., De Neve, H., & Weisbuch, C. Impact of planar microcavity effects on light extraction-Part I: basic concepts and analytical trends. *IEEE J. Quantum Elect.* **34** (9), 1612-1631 (1998).
34. Köhler, A. Ein neues Beleuchtungsverfahren für mikrophotographische Zwecke. *Zeitschrift für wissenschaftliche Mikroskopie und für Mikroskopische Technik.* **10** (4), 443-440 (1893).
35. Köhler, A. New method of illumination for photomicrographical purposes. *Journal Royal Microscopical Society (Great Britain)*. **14**, 261-262 (1894).
36. He, Y.-M. *et al.* On-demand semiconductor single-photon source with near-unity indistinguishability. *Nat. Nanotechnol.* **8** (3), 213-217 (2013).

Copyright © 2017 Journal of Visualized Experiments